Solution of the Phase Change Stefan Problem With Time-Dependent Heat Flux Using Perturbation Method

Mohammad Parhizi

Mechanical and Aerospace Engineering Department,
University of Texas at Arlington,
500 W First Street, Room 211,
Arlington, TX 76019

Ankur Jain[1]

Mechanical and Aerospace Engineering Department,
University of Texas at Arlington,
500 W First Street, Room 211,
Arlington, TX 76019
e-mail: jaina@uta.edu

Theoretical understanding of phase change heat transfer problems is of much interest for multiple engineering applications. Exact solutions for phase change heat transfer problems are often not available, and approximate analytical methods are needed to be used. This paper presents a solution for a one-dimensional (1D) phase change problem with time-dependent heat flux boundary condition using the perturbation method. Two different expressions for propagation of the phase change front are derived. For the special case of constant heat flux, the present solution is shown to offer key advantages over past papers. Specifically, the present solution results in greater accuracy and does not diverge at large times unlike past results. The theoretical result is used for understanding the nature of phase change propagation for linear and periodic heat flux boundary conditions. In addition to improving the theoretical understanding of phase change heat transfer problems, these results may contribute toward design of phase change based thermal management for a variety of engineering applications, such as cooling of Li-ion batteries. [DOI: 10.1115/1.4041956]

1 Introduction

A fundamental understanding of heat transfer processes during phase change is critical for optimizing multiple engineering applications where melting and solidification occurs, such as metal casting, thermal management, process manufacturing, etc. [1,2]. Heat transfer in an engineering system involving phase change requires the modeling of heat absorption or release at the phase change front, the location of which usually changes with time [3]. In general, such problems are nonlinear in nature, although engineering approximations are often made in order to linearize and solve these problems [1–4]. The Stefan number, defined as $Ste = C_p(T_{ref} - T_m)/L$, which represents the ratio of sensible heat to latent heat, is a key nondimensional parameter in such problems. The simplest phase change problem involves a one-dimensional (1D), semi-infinite body, initially at the melting temperature, T_m, being heated up or cooled down by a constant temperature, T_0 imposed at its end. This problem, often referred to as the Stefan problem has a standard solution, which shows that the location of the phase change front, $Y(\tau)$ is proportional to $\sqrt{\alpha \tau}$ where α is the thermal diffusivity [5]. Several variants of this problem have been addressed in past work, including a heat flux boundary condition [6–11], convective flow within the melted liquid [12,13], time-dependent temperature boundary condition [14–16], convective boundary condition [8], phase change over a temperature range [17], etc. Only the simplest of these phase change problems admits an exact solution—in most other cases, one must resort to approximate analytical methods that often result in series solutions.

A number of approximate solution methods are available for solving phase change problems [2,18]. For example, the perturbation method has been used to solve the problem with a time-dependent boundary condition [14,15] as well as a problem with a constant heat flux boundary condition [8]. This method involves expressing the temperature distribution as a series solution involving powers of the Stefan number, and solving for each term individually. Solving for only the first few terms of the series provides a reasonably accurate solution, particularly for small values of *Ste*. Integral methods apply the heat balance integral to phase change problems, similar to the momentum integral in boundary layer theory [19] and have been used for solving phase change problems with time-dependent temperature boundary conditions [3,19]. Quasi-stationary and quasi-steady methods have also been used [3]. These methods are particularly applicable if the solid–liquid interface location moves slowly and the transient term in the energy equation can be neglected. While much of the work in this direction addresses cases with temperature boundary condition, relatively lesser work exists on analysis of heat flux boundary condition. This problem has been solved for the specific cases of constant heat flux using the integral method [6] and by approximating the form of the temperature distribution [7]. A series solution has been derived for the specific case of a sinusoidal boundary condition [8]. Solution for the problem with time-dependent heat flux has been derived using a series solution [11] as well as expansion of the temperature distribution as a function of the error integral family [9]. A few highly mathematical treatments of such problems also exist, including proofs for existence and uniqueness of solutions for nonlinear Stefan problems [20,21], although these results are difficult to apply for engineering problems.

This paper presents a theoretical analysis of the problem of one-dimensional phase change involving a time-dependent heat flux boundary condition using a perturbation method. Time-dependent heat flux may be encountered when, for example, a heat-generating body such as a Li-ion cell undergoing high rate discharge is being cooled by a phase change material. In this case, heat flux entering the phase change material may change with time due to time-dependent heat generation and transient thermal conduction within the Li-ion cell [22]. In this work, this problem is solved by expanding the temperature distribution in a power series involving the Stefan number and solving for the first three terms of the power series. Comparison of the theoretical results with past papers is presented. For a specific case of constant heat flux, results from this work are shown to be close to results from past papers that utilized other methods. The present work is shown to be able to accurately predict the time evolution of the phase change front at large times, while several past models are found to diverge. Results are found to be in good agreement with finite element simulation results, while providing significant advantage in terms of computational time. The analytical method is used for analyzing the dependence of the solution on key thermal parameters. These results contribute towards an improved theoretical understanding of a heat transfer problem that is commonly encountered in multiple engineering applications.

2 Mathematical Modeling

Consider a one-dimensional, semi-infinite body initially at its phase change temperature T_m. Figure 1 shows this schematically for the specific case of solid-to-liquid phase change, although the

---
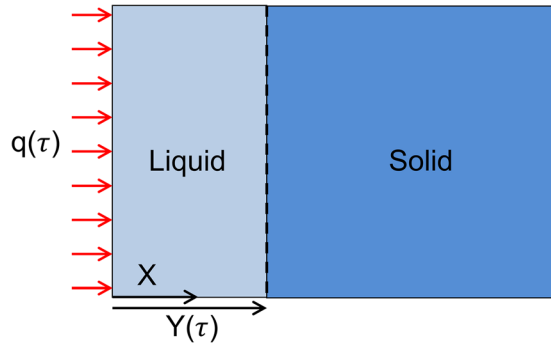
Fig. 1 Schematic of the one-dimensional phase change problem with time-dependent heat flux. The schematic shows solid-to-liquid phase change, but the opposite process can also be analyzed in the same framework.

reverse process of liquid-to-solid phase change can also be analyzed using the results derived in this section. Heat flux at the $X = 0$ end is a known function of time, $q(\tau)$. Heat enters the body with time, resulting in phase change and propagation of the phase change front with time. A key quantity of interest in such a problem is the location of the solid–liquid interface as a function of time, $Y(\tau)$. In addition, temperature distribution within the newly formed phase, $T(X,\tau)$ is also of interest. Convection in the liquid phase is neglected. Following the nondimensionalization of variables as summarized in the Nomenclature section, the temperature field must satisfy the following governing energy conservation equation:

$$\frac{\partial^2 \theta}{\partial x^2} = \frac{\partial \theta}{\partial t} \tag{1}$$

where $x > 0$ and $t > 0$.

$\theta(x,t)$ is subject to the following boundary condition:

$$-\frac{\partial \theta}{\partial x} = g(t) \quad \text{at } x = 0 \tag{2}$$

where $g(t)$ is the nondimensional temperature gradient at the boundary.

Temperature continuity and energy conservation at the solid–liquid interface requires that

$$\theta = 0 \quad \text{at } x = y(t) \tag{3}$$

and

$$-Ste\left[\frac{\partial \theta}{\partial x}\right]_{x=y(t)} = \frac{dy}{dt} \quad \text{at } x = y(t) \tag{4}$$

In order to determine the unknown phase change front $y(t)$ and the temperature distribution following phase change $\theta(x,t)$, Eq. (1) is transformed in order to replace t with y as an independent variable. By doing so, Eq. (1) results in

$$\frac{\partial^2 \theta}{\partial x^2} = -Ste \frac{\partial \theta}{\partial y}\left[\frac{\partial \theta}{\partial x}\right]_{x=y} \tag{5}$$

The boundary condition at $x = 0$ is rewritten in terms of y as follows:

$$-\frac{\partial \theta}{\partial x} = g(t) = G(y) \quad \text{at } x = 0 \tag{6}$$

In order to solve this problem for time-varying $g(t)$, the temperature distribution $\theta(x,y)$ is written in the form of a series involving the first three powers of Ste, similar to past papers that utilized this approach for a time-dependent temperature boundary condition [14,15]

$$\theta(x,y) = \theta_0(x,y) + Ste \times \theta_1(x,y) + Ste^2 \times \theta_2(x,y) \tag{7}$$

By substituting Eq. (7) into Eq. (5), governing equations and associated boundary conditions for the temperature components $\theta_0(x,y)$, $\theta_1(x,y)$, and $\theta_2(x,y)$ can be derived. These ordinary differential equations can be solved to result in the following solution:

$$\theta_0(x,y) = -G(y)(x - y) \tag{8}$$

$$\theta_1(x,y) = G(y)\left[-G'(y)\left(\frac{x^3 - y^3}{6}\right) + \left(G(y) + G'(y)y\right)\left(\frac{x^2 - y^2}{2}\right)\right] \tag{9}$$

$$\theta_2(x,y) = \frac{A}{20}\left(x^5 - y^5\right) + \frac{B}{12}\left(x^4 - y^4\right) + \frac{C}{6}\left(x^3 - y^3\right) + \frac{D}{2}\left(x^2 - y^2\right) \tag{10}$$

where

$$A = -\frac{1}{6}G(y)\left(G'^2(y) + G''(y)G(y)\right) \tag{11}$$

$$B = \frac{1}{2}G(y)\left(y\left(G'^2(y) + G''(y)G(y)\right) + 3G(y)G'(y)\right) \tag{12}$$

$$C = G(y)G'(y)\left[y\left(yG'(y) + G(y)\right) - G'(y)\frac{y^2}{2}\right] \tag{13}$$

Note that the forcing function $G(y)$ is assumed to be appropriately differentiable.

The location of the phase change front, $y(t)$ in Eqs. (8)–(14) is unknown. In order to solve for $y(t)$, energy balance at the interface is utilized. Substituting Eqs. (7)–(14) in Eq. (4) results in

$$D = \left[\begin{array}{l} -G(y)\left(yG'(y) + G(y)\right)\left(y\left(yG'(y) + G(y)\right) - G'(y)\frac{y^2}{2}\right) \\ + G(y)\left(-2G(y)G'(y)y^2 - yG^2(y) - \frac{1}{3}y^3\left(G'^2(y) + G''(y)G(y)\right)\right) \end{array}\right] \tag{14}$$

$$\frac{dy}{dt} = -Ste\left[\begin{array}{l} -G(y) + Ste \times G(y)\left(\left(yG'(y) + G(y)\right)y - G'(y)\frac{y^2}{2}\right) \\ + Ste^2\left(\frac{A}{4}y^4 + \frac{B}{3}y^3 + \frac{C}{2}y^2 + Dy\right) \end{array}\right] \tag{15}$$

Finally, as is the case in perturbation analysis [14,15], derivatives of G are neglected, and the following nonlinear ordinary differential equation is obtained for $y(t)$:

$$y' + Ste^2 G^2(y)y - 2Ste^3 G^3(y)y^2 = (Ste)G(y) \qquad (16)$$

For cases with relatively simple expression for the heat flux, this equation can be directly solved. In general, a solution for $y(t)$ can be derived by neglecting the Ste^3 term, which may be reasonable since $Ste \ll 1$. In such a case, the general solution for $y(t)$ is found to be

$$y(t) = \left(\int Ste \times g(t^*) \exp\left(\int Ste^2 g^2(t^{**})dt^{**} \right) dt^* + C \right)$$
$$\times \left(\exp\left(-\int Ste^2 g^2(t^*)dt^* \right) \right) \qquad (17)$$

where C is a constant which is determined using the initial condition of $y(0) = 0$. The temperature distribution $\theta(x,y)$ can be determined by substituting $y(t)$ from Eq. (17) into Eqs. (7)–(14).

This completes the derivation of solution of the problem with time-dependent heat flux using perturbation method. Due to approximations made during the derivation, this solution is valid only for small values of Ste, which is usually appropriate for materials of engineering interest due to the relatively large value of the enthalpy of phase change compared to specific heat. Further, note that since the previous derivation involves derivatives of the forcing function $G(y)$, the approach utilized here may not be appropriate in the case of a heat flux profile that is not appropriately differentiable.

Comparison of these results with past work, particularly for the specific case of constant heat flux is analyzed next.

3 Results and Discussion

In order to compare with results from past work [9,10,19], it is instructive to examine the solution presented here when the heat flux is constant, for which, solutions based on other methods are available. There are two distinct approaches for simplifying the general treatment in Sec. 2 and deriving the solution for the phase change front when $g(t) = g_0$.

First, for constant heat flux, Eq. (16) can be shown to have an exact solution, given by

$$y(t) = \frac{\sqrt{7} \tan\left(\frac{1}{2}\sqrt{7}\gamma^2 t - \tan^{-1}\left(\frac{1}{\sqrt{7}} \right) \right) + 1}{4\gamma} \qquad (18)$$

where

$$\gamma = Ste \times g_0 \qquad (19)$$

Alternately, the integral in Eq. (17) can be computed for the case of constant heat flux to result in the following solution:

$$y(t) = \gamma t - \frac{1}{2}\gamma^3 t^2 + \frac{1}{6}\gamma^5 t^3 - \frac{1}{24}\gamma^7 t^4 + \frac{1}{120}\gamma^9 t^5 - \frac{1}{720}\gamma^{11}t^6 \ldots \qquad (20)$$

While Eq. (18) represents the general solution for the constant heat flux case, Eq. (20) is based on neglecting higher order terms in Eq. (16). Note that the solution in Eq. (18) is not valid for large t where the tan function may diverge, which is the case for the past work as well. On the other hand, Eq. (20) does not have such a restriction and converges uniformly even at large times.

Equation (20) offers a good physical insight into the solution. The first term in Eq. (20) represents the rate of heat absorption at the phase change interface, and further terms represent the effect of sensible heat in the newly formed phase. In many engineering cases, where latent heat dominates over sensible heat, heat absorption in the newly formed phase can be neglected, and only the first term of this equation may be sufficient.

It is instructive to compare the solutions derived here, Eqs. (18) and (20) with results from past papers that have presented solutions for the constant heat flux case. Specifically, the solution for the phase change front has been derived by Tao [9], Goodman [19], and Carslaw and Jaegar [10] as follows:

$$y(t) = \gamma t - \frac{1}{2}\gamma^3 t^2 + \frac{5}{6}\gamma^5 t^3 - \frac{17}{18}\gamma^7 t^4 + \frac{827}{120}\gamma^9 t^5 \ldots \qquad (21)$$

$$y(t) = \gamma t - \frac{1}{2}\gamma^3 t^2 + \frac{5}{6}\gamma^5 t^3 - \frac{17}{18}\gamma^7 t^4 + \frac{795}{120}\gamma^9 t^5 \ldots \qquad (22)$$

$$y(t) = \gamma t - \frac{1}{2}\gamma^3 t^2 + \frac{5}{6}\gamma^5 t^3 \ldots \qquad (23)$$

While Eq. (21) was derived by Tao by expressing temperature in terms of polynomial functions of error integrals [9], Eq. (22) was derived by Goodman using the heat balance integral method [19]. Eq. (23) was derived by Carslaw and Jaegar by writing $y(t)$ as a power series [10].

It can be seen that the expression for the phase change front derived in this work for the specific case of constant heat flux by neglecting the Ste^3 term, Eq. (20) is close to results from several papers that solved the same problem using other techniques. The first two terms are identical, with a departure occurring in the third term. Figure 2(a) plots $y(t)$ as a function of t derived in this work (Eqs. (18) and (20)) and compares with past papers [9,10,19] as well as numerical computation based on finite element method (FEM) for a nondimensional, constant $g_0 = 5000$. In this case, the enthalpy method is used in the finite element simulations for solving for computing temperature distribution in the phase change material, which is defined as a binary mixture of liquid and solid.
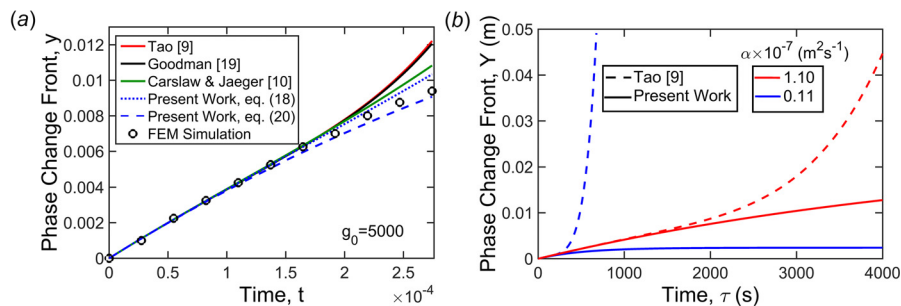
Fig. 2 Comparison of the present analytical result with past results for the special case of constant heat flux: (a) plot of nondimensional phase change front location, $y(t)$ as a function of nondimensional time, t for the present work and three past results [9,10,19]. Results from FEM simulation are also shown for comparison. (b) Comparison of present model with Tao [9] for a larger time period for two different values of α.
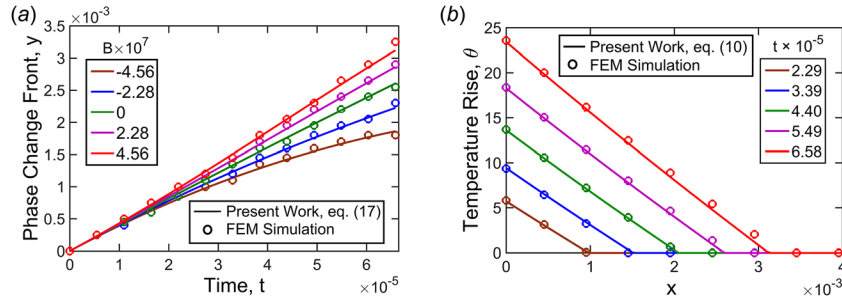
Fig. 3 Validation of the present work with finite element simulation for linear, time-varying heat flux: (a) phase change front $y(t)$ as a function of t for linear $g(t) = A + Bt$. The value of A is taken to be 5000 and values of B are shown in the legend. (b) Temperature distribution as a function of x for the specific case of $B = 4.56 \times 10^7$. Both plots show very good agreement between the analytical model and finite element simulation.

The FEM simulation is validated separately against the analytical solution of the well-known Stefan problem with constant temperature boundary condition. Mesh independence is also ensured. Very good agreement with past papers is seen up to a nondimensional time of around 2.5×10^{-4}. As time increases, solutions from past studies lose accuracy beyond around $t = 2.5 \times 10^{-4}$, while the present result continues to agree well with finite element simulations. Figure 2(b) investigates this further by plotting the phase change front $Y(\tau)$ over a much larger time range, up to $\tau = 4000\,s$ for different values of thermal diffusivity. This plot is shown in dimensional form since plotting in nondimensional form would not be appropriate as thermal diffusivity influences both t and $y(t)$. It is clearly seen that previous models diverge and fail to accurately predict $Y(\tau)$ at large times, beyond around $\tau = 1500\,s$ for $\alpha = 1.10 \times 10^{-7}$ m^2/s. While the convergence of past models can be improved by including many more terms [3], derivation of further terms for these models is very cumbersome and impractical [3,9]. While Eq. (18) may also diverge at large times due to the presence of the tan function, Eq. (20) in the present work clearly converges even at large times, even with a few number of terms. Computation of terms further than those shown in Eq. (20) is also simpler than past work.

It has been shown [3] that the result from Tao [9], shown in Eq. (21), is valid only when the nondimensional parameter $\beta = (q^2/\rho^2\alpha L^2)\tau$ is less than 0.4. This explains why the solution by Tao [9], Eq. (21), diverges at large times. This also explains divergence at even smaller times when computed for larger value of α, as shown in Fig. 2(b). On the other hand, the present solution, Eq. (20), does not suffer from such divergence problems and continues to predict the interface location even at large times. This represents a key advantage of the present technique compared to past work.

Note that in Fig. (2), the value of the reference length for nondimensionalization is taken to be $b = 1$ m. Further, the value of Stefan number is 0.008 based on $T_{ref} - T_m = 1$ K and thermal properties of commercial paraffin wax.

For further validation of the theoretical results, the phase change front $y(t)$ is plotted in Fig. 3(a) as a function of time based on Eq. (17) assuming linear $g(t) = A + Bt$. While the value of A is held constant at 5000, a number of cases with different values of B are considered in order to investigate the effect of the slope of $g(t)$. The values of b and Ste are the same as in Fig. 2. Results from FEM computations are also plotted in Fig. 3(a) for comparison. Further, Fig. 3(b) plots the temperature distribution in the newly formed phase at different times for a specific input heat flux, with $A = 5000$ and $B = -4.56 \times 10^7$. Figure 3(a) shows very good agreement between the analytical solution and FEM-based computations for each heat flux considered. As the value of B increases, the nature of $y(t)$ curves changes from concave to convex, which is along expected lines, since an increase in the value of B results in more heat flux into the medium, and therefore, a greater rate of propagation of the phase change front. There is also very good agreement in the temperature distribution at multiple times, as shown in Fig. 3(b). Note that the analytical solution is significantly faster than finite element simulation since the solution is obtained as a closed form equation and does not require time-intensive discretization and solution of a large system of equations.

Periodic heat flux boundary conditions are of interest in a variety of applications. Figure 4(a) presents computed profiles of the solid–liquid interface as a function of time for periodic, $g(t) = A(1 + \cos(\varepsilon t))$, where $\varepsilon = \omega b^2/\alpha$ is the nondimensional frequency. The values of b and Ste are the same as in Fig. 2, and $A = 5000$. Figure 4(a) shows that the theoretical model presented
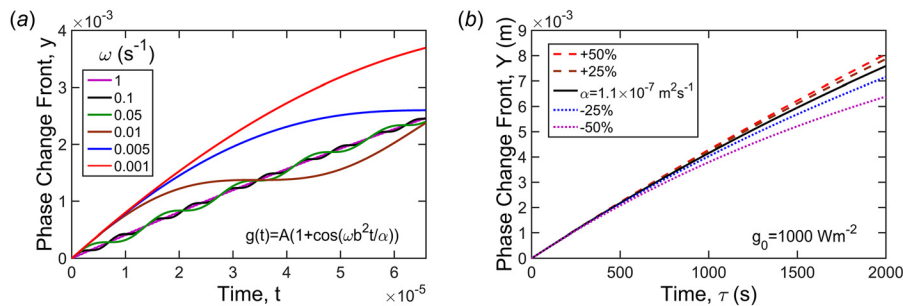
Fig. 4 (a) Plot of phase change front $y(t)$ as a function of time for periodic $g(t) = A(1+\cos(\varepsilon t))$ for multiple values of the nondimensional frequency, ε. (b) Plot of the variation in phase change front propagation for different values of thermal diffusivity for constant heat flux case.

in this work is able to capture the time evolution of the phase change front for different frequencies. The number of oscillations within the time period considered decreases as frequency decreases, as expected.

It is of interest to examine the dependence of the solution on the value of thermal diffusivity, which is a key thermophysical property that governing phase change propagation. Figure 4(b) plots phase change front as a function of time for multiple values of thermal diffusivity α. Figure 4(b) considers up to $\pm 50\%$ variation in thermal diffusivity from the baseline value of 1.1×10^{-7} m^2/s, which is the typical value of thermal diffusivity of paraffin wax used for multiple phase change heat transfer applications. This plot indicates that an increase in thermal diffusivity results in a slight increase in $y(t)$. This happens because of more rapid heat transfer through the newly formed phase at a higher value of thermal diffusivity, and vice versa. Unlike the case of constant temperature boundary condition, where the phase change front location is known to be proportional to $\sqrt{\alpha\tau}$ [3,4], a similar explicit relationship is not available for heat flux boundary conditions.

Time-varying heat flux in a phase change problem can be encountered in applications where a phase change material cools down a heat-generating body in which the heat generation itself is a function of time. For example, phase change cooling of Li-ion cells has been of much recent research attention [22,23]. Since heat generation in Li-ion cells changes with time as the electrical load changes [24]; therefore, heat flux into the phase change material is also likely to change with time. For such applications, the present model offers a theoretical framework for thermal analysis and optimization. While the perturbation method used here does not apply for very short times, such information is often not important for engineering analysis.

Extension of the treatment discussed here to problems in cylindrical and spherical coordinate systems, which may also have practical applications, is reasonably straightforward, following the same approach as Eqs. (7)–(17) to account for the time-dependent heat flux.

4 Conclusions

This work presents a solution for the phase change heat transfer problem with time-dependent heat flux boundary condition using the perturbation method. The solution is shown to converge at large times, where solutions from past papers are known to diverge. This represents a significant improvement in our theoretical understanding of phase change heat transfer. The theoretical results presented here may be relevant to multiple engineering applications, such as cooling of Li-ion cells. Results derived here are used to understand the effect of linear and periodic heat flux boundary conditions, which may arise in such applications. These results can be easily extended to cylindrical and spherical coordinate systems.

Acknowledgment

Nomenclature

b = reference length scale (m)
C_p = specific heat capacity (J/kg K)
g = nondimensional boundary condition, $g = qb/k(T_{\text{ref}} - T_m)$
k = thermal conductivity (W/mK)
L = latent heat of fusion (J/kg)
q = heat flux (W/m^2)
Ste = Stefan number, $Ste = C_p(T_{\text{ref}} - T_m)/L$
t = nondimensional time, $t = \alpha\tau/b^2$
T = temperature (K)
T_m = phase change temperature (K)
T_{ref} = reference temperature (K)
x = nondimensional lengthscale, $x = X/b$
X = lengthscale (m)
y = nondimensional location of phase change front, $y = Y/b$
Y = location of phase change front (m)
α = thermal diffusivity (m^2/s)
θ = nondimensional temperature, $\theta = (T - T_m)/(T_{\text{ref}} - T_m)$
ε = nondimensional frequency, $\varepsilon = \omega b^2/\alpha$
τ = time (s)
ω = frequency (1/s)

References

[1] Viskanta, R., 1988, "Heat Transfer During Melting and Solidification of Metals," ASME J. Heat Transfer, 110(4b), pp. 1205–1219.

[2] Fukusako, S., and Seki, N., 1987, "Fundamental Aspects of Analytical and Numerical Methods on Freezing and Melting Heat-Transfer Problems," Annu. Rev. Heat Transfer, 1(1), pp. 351–402.

[3] Cheng, K. C., and Seki, N., eds., 1991, Freezing and Melting Heat Transfer in Engineering: Selected Topics on Ice-Water Systems and Welding and Casting Processes, CRC Press, Boca Raton, FL.

[4] Stefan, J., 1891, "Uber Die Theorie Des Eisbildung, Insbesonder Uber Die Eisbildung im Polarmere," Ann. Phys., 42(2), pp. 269–286.

[5] Hahn, D. W., and Özişik, M. N., 2012, Heat Conduction, 3rd ed., Wiley, Hoboken, NJ.

[6] Ruehr, O. G., 2002, "Analytical-Numerical Treatment of the One-Phase Stefan Problem With Constant Applied Heat Flux," Integral Methods in Science and Engineering, Birkhäuser, Boston, MA, pp. 215–220.

[7] Cho, S. H., and Sunderland, J. E., 1981, "Approximate Temperature Distribution for Phase Change of a Semi-Infinite Body," ASME J. Heat Transfer, 103(2), pp. 401–403.

[8] Gutman, L. N., 1986, "On the Problem of Heat Transfer in Phase-Change Materials for Small Stefan Numbers," Int. J. Heat Mass Transfer, 29(6), pp. 921–926.

[9] Tao, L. N., 1979, "On Free Boundary Problems With Arbitrary Initial and Flux Conditions," Z. Angew. Math. Phys., 30(3), pp. 416–426.

[10] Carslaw, H. S., and Jaeger, J. C., 1986, Conduction of Heat in Solids, Oxford Science Publications.

[11] Evans, G. W., Isaacson, E., and MacDonald, J. K. L., 1950, "Stefan-Like Problems," Q. Appl. Math., 8(3), pp. 312–319.

[12] Szekely, J., and Stanek, V., 1970, "Natural Convection Transients and Their Effects on Unconditional Solidification," Metall. Trans., 1(1), pp. 2243–2251.

[13] Cole, G. S., and Winegard, W. C., 1962, "Thermal Convection Ahead of a Solid-Liquid Interface," Can. Metall. Q., 1(1), pp. 29–31.

[14] Lock, G., Gunderson, J., Quon, D., and Donnelly, J., 1969, "A Study of One-Dimensional Ice Formation With Particular Reference to Periodic Growth and Decay," Int. J. Heat Mass Transfer, 12(11), pp. 1343–1352.

[15] Caldwell, J., and Kwan, Y., 2003, "On the Perturbation Method for the Stefan Problem With Time-Dependent Boundary Conditions," Int. J. Heat Mass Transfer, 46(8), pp. 1497–1501.

[16] Tao, L. N., 1978, "The Stefan Problem With Arbitrary Initial and Boundary Conditions," Q. Appl. Math., 36(3), pp. 223–233.

[17] Tien, R. T., 1965, "Freezing of Semi-Infinite Slab With Time Dependent Surface Temperature—An Extension of Neumann's Solution," Trans. AIME, 233, pp. 1887–1891.

[18] Mori, A., and Araki, K., 1976, "Methods for Analysis of the Moving Boundary-Surface Problem," J. Math. Anal. Appl., 16(4), pp. 734–744.

[19] Goodman, T. R., 1958, "The Heat Balance Integral and Its Application to Problems Involving Change of Phase," Trans. ASME, 80(2), pp. 335–342.

[20] Cannon, J., and Primicerio, M., 1971, "Remarks on the One-Phase Stefan Problem for the Heat Equation With the Flux Prescribed on the Fixed Boundary," J. Math. Anal. Appl., 35(2), pp. 361–373.

[21] Kyner, W., 1959, "An Existence and Uniqueness Theorem for a Nonlinear Stefan Problem," Indiana Univ. Math. J., 8(4), pp. 483–498.

[22] Shah, K., Vishwakarma, V., and Jain, A., 2016, "Measurement of Multiscale Thermal Transport Phenomena in Li-Ion Cells: A Review," ASME J. Electrochem. Energy Convers. Storage, 13(3), p. 030801.

[23] Ling, Z., Zhang, Z., Shi, G., Fang, X., Wang, L., Gao, X., Fang, Y., Xu, T., Wang, S., and Liu, X., 2014, "Review on Thermal Management Systems Using Phase Change Materials for Electronic Components, Li-Ion Batteries and Photovoltaic Modules," Renewable Sustainable Energy Rev., 31, pp. 427–438.

[24] Anthony, D., Wong, D., Wetz, D., and Jain, A., 2017, "Non-Invasive Measurement of Internal Temperature of a Cylindrical Li-Ion Cell During High-Rate Discharge," Int. J. Heat Mass Transfer, 111, pp. 223–231.